HHS Public Access

Author manuscript

Laryngoscope. Author manuscript; available in PMC 2015 March 18.

Published in final edited form as:

Laryngoscope. 2014 March ; 124(3): 649–654. doi:10.1002/lary.24321.

Nasal tip support: A finite element analysis of the role of the caudal septum during tip depression

Cyrus T. Manuel, BS[1,*], **Ryan Leary, BA**[1,*], **Dmitriy E. Protsenko, PhD**[1], and **Brian J.F. Wong, MD, PhD**[1,2,3]

[1]Beckman Laser Institute, University of California Irvine, Irvine, California 92612

[2]Department of Biomedical Engineering, 3120 Natural Sciences II, University of California Irvine, Irvine, California 92612

[3]Department of Otolaryngology, Head and Neck Surgery, University of California Irvine, Orange, California 92868

Abstract

Objective/Hypothesis—Although minor and major tip support mechanisms have been described in detail, no quantitative models exist to provide support for the relative contributions of the structural properties of the major alar cartilage, the fibrous attachments to surrounding structures, and the rigid support structures in an objective manner.

Study Design—The finite element method was used to compute the stress distribution in the nose during simple tip compression, and then identify the specific anatomic structures that resist deformation and thus contribute to “tip support”. Additionally, the impact of caudal septal resection on nasal tip support was examined.

Method—The computer models consisted of three tissue components with anatomically correct geometries for skin and bone derived from CT data. Septum, upper lateral cartilages, and major alar cartilages were fitted within the model using 3D CAD software. 5mm nasal tip compression was performed on the models with caudal septal resection (3mm and 5 mm) and without resection to simulate palpation, then the resulting spatial distribution of stress and displacement was calculated.

Results—The von Mises stress in the normal model was primarily concentrated along medial crural angle. As caudal septum length was reduced, stress was redistributed to adjacent soft tissue and bone, resulting in less force acting on the septum. In all models, displacement was greatest near the intermediate crura.

Conclusions—These models are the first step in the comprehensive mechanical analysis of nasal tip dynamics. Our model supports the concept of the caudal septum and major alar cartilage as providing the majority of critical load-bearing support.

Address correspondence to Brian J.F. Wong, MD, PhD Beckman Laser Institute, University of California Irvine, 1002 Health Sciences Road, Irvine, California 92612, USA; Telephone: (949) 824-7997; Fax: (949) 824-8413; bjwong@uci.edu.

*Senior Authors

Financial Disclosure:

Conflict of interest: None

Level of Evidence—N/A

Keywords

Otolaryngology; Rhinoplasty; Reconstructive Surgery; Finite Element Modeling; nasal tip support

INTRODUCTION

When operating on the nasal tip, the rhinoplasty surgeon must balance maneuvers that increase structural support with those that enhance aesthetics and preserve the airway. Intimate knowledge of major and minor nasal tip support mechanisms is essential for optimal long-term outcomes. Current understanding of nasal tip support mechanisms is derived largely from clinical experience[1,2]; however, these mechanisms and their relative contributions have yet to be objectively verified using rigorous quantitative methods.

Currently, finite element model (FEM) use to study the organs of head, neck, and upper airway has been focused primarily on the examination of middle ear mechanics, load distribution in the facial bones, or laryngeal biomechanics[3–5]. Modeling of the nose and nasal tip receives only modest attention. At present, studies of nasal biomechanics have focused largely on analysis of septal buckling under extreme loading conditions[6,7], and these forces are quite different from those encountered during such maneuvers as palpation of the nasal tip or the sustained forces produced by wound contracture or even gravity. Palpation of the nasal tip is the rhinoplasty surgeon's most valuable means to subjectively gauge nasal tip support and stability. Although these prior FEM studies provided insight with respect to understanding the main support structure of nasal dorsum, they each fall short by failing to incorporate the major alar and upper lateral cartilages in their structural simulation, which are well known to provide major tip support under both static and dynamic loading conditions.

In this study, we developed a multi-component, anatomically realistic nasal tip FEM aimed at providing estimates of the stress distribution in the nasal tip when depressed. An accurate digital model of the human nose was created, consisting of bone, cartilage, and soft tissue envelope (skin) components. Accordingly, the FEM calculated the internal stress distribution within the nasal tip structures in response to simple depression. As a test of the potential applications of this model, two simulations of varying caudal septal resection/trim (3mm and 5mm) were created to emulate the time-honored approach to creating tip rotation during endonasal rhinoplasty. Our multi-component finite element model is the first step in developing a detailed model that may describe the mechanical changes in overall nasal structural dynamics in response to various maneuvers in modern rhinoplasty.

METHODS

Construction of the Finite Element Models

The finite element model was constructed from a high-resolution computed tomography (CT) scan of a single patient and with 3D computer-aided design (CAD) software. This study was performed in accordance with the guidelines of the institutional review board

(IRB) at University of California, Irvine. The overall workflow for model construction process is demonstrated in Figure 1. The segmentation, surface reconstruction, and assembly of all three components (bone, cartilage, and soft tissue) were executed in Mimics (Materialise, Plymouth, MI), with the exception of building and designing the cartilage structures. Mesh generation and editing was performed in 3-Matic (Materialise, Plymouth, MI) and then imported in COMSOL Multiphysics (Los Angeles, CA) where material properties and boundary conditions were assigned.

The geometry of the soft tissue and bone components were segmented by thresholding in Mimics. Surface reconstructions of the soft tissue and bone were verified and exported in the Standard Tessellation Language format (STL) to be used as reference for the reconstruction of the cartilage anatomy. Since cartilage has the same density as soft tissue in computed tomography, segmentation by thresholding is not possible. Thus, 3D CAD software and Mimics were necessary to construct de novo anatomically correct septal, upper lateral, and the lower alar cartilages. These cartilaginous structures were customized to fit within the soft tissue envelope of our model. The normal septum was drawn in Mimics using orthogonal views in the computed tomography scan as a guide. Subsequently, the 3D-editing function in Mimics was used to trim the caudal portion of the septum in a manner emulating that of a classic endonasal rhinoplasty. A 3mm caudal septal trim was simulated to mimic the effects of this common endonasal rhinoplasty maneuver and a 5mm caudal trim model was constructed to demonstrate the effects of an excessive resection, which obviously would not be performed clinically.

The major alar cartilage geometry, in contrast, was based on measurements taken from a human cadaveric tissue specimen and from observations of multiple open rhinoplasty operations of the senior author to approximate real anatomy. Cadaveric major alar cartilages were obtained and traced onto paper to ensure proper size and proportions in accord with IRB guidelines. The tracings were digitally scanned and imported into 3D Max software (Autodesk, San Rafael, CA) in addition to the STL surface of the soft tissue and bone as described above. Polygons were used to construct a model that was fitted to the 2D tracing, and then the polygons were extruded to create thickness. In vivo measurements of medial, intermediate, and lower lateral crura of patients during rhinoplasty surgery were taken to adjust size, orientation, and geometry of the major alar cartilage for the model. Upper lateral cartilages were constructed using the soft tissue as an envelope and made to fit within skin envelope of lateral nasal wall of the model[8]. The final multi-component model is shown in Figure 2.

Analysis in COMSOL

Finite element models were created in COMSOL Multiphysics and assigned linear and isotropic properties for skin, cortical bone and cartilage. The material properties used in these models are listed in (Table 1) and taken from the literature[7, 9–13]. Physical properties of skin, including the mass density and Poisson's ratio, were approximated and applied to the soft tissue envelope[14]. Articular cartilage mechanical properties were used in this model due to the sparse information and limited quality of the data on the mechanical properties of facial cartilage. To be as realistic as possible, the bone in the model was fixed and the rest of

the cartilage and overlying skin was free to move. A $10mm^2$ surface as indicated in Figure 3 was prescribed a displacement 5mm in the posterior direction to simulate nasal tip palpation in COMSOL Multiphysics. The resulting von Mises stress and strain of each model were calculated. von Mises stress is a scalar value that combines the normal and shear stresses under a complex 3D loading condition. It can be used to determine whether a material will undergo elastic or plastic deformation. If the von Mises stress exceeds the yield stress of the material, also a scalar value determined from a uniaxial tension test, the material will behave like plastic and permanently deform. This von Mises yield criterion is often used in engineering to determine whether an isotropic and ductile material will yield under complex loading conditions; in this case, nasal tip depression. In subsequent text, when the term "stress" is used, we are referring to the von Mises values.

The key load-bearing and displaced structures within the nose were identified by examining results from the computer simulations. By identifying these key regions, we determined the structures that are most resistant to deformation and thus are the greatest contributors to structural support of the nasal tip. Since the tip is a heterogeneous composite structure, the FEM approach is the most straightforward method of obtaining an estimate.

Accompanying the identification of nasal tip support structures, the recoil force of the entire model was determined in all finite element models. The force of nasal tip recoil, which is estimated subjectively during the physical exam, was calculated by integrating the uniaxial reaction force (the force that opposes the nasal tip depression) over cartilage components positioned against bone. This analysis was utilized to validate the consistency of the models' behavior with what is observed in the clinical exam; that is, we expect a decrease in recoil force as more cartilage is resected from the caudal septum.

RESULTS

Stress Distribution

The representative spatial distribution of stress for each of the three conditions (0mm, 3mm, and 5mm caudal septal resection) is shown in Figure 4. The key load-bearing cartilaginous structures, highlighted in dark red, are primarily located at the junction of the medial crural angle bilaterally as well as the caudal portion of the septal cartilage. Of note, the caudal portion of the upper lateral cartilage and the cephalic portion of the lower lateral cartilage were affected; however, the stress increase was not as dramatic. Additionally, regions of stress were located at the junction of the cartilaginous septum and the perpendicular plate as well as the lateral inferior portion of the nasal bones along the junction with the upper lateral cartilages.

As the major rigid support structure of the nose, the septum had the highest concentration of stress located in its most caudal portion when the nasal tip is depressed (Figure 5a). Much of this load-bearing region was removed after the 3mm reduction (Figure 5b) and nearly the entire region was removed with the 5mm reduction (Figure 5c). Volumetric integration of von Mises stresses in septum with 0mm resection, 3mm resection, and 5mm resection are 0.0286N*m, 0.0273N*m, and 0.0235N*m respectively. The total von Mises stress integrated across the entire septum was reduced by 4.5% in the 3mm caudal trim model

compared to normal. Consequently, the 5mm caudal trim model resulted in a 17.8% reduction in total stress when compared with the normal model. It is also important to note that the recoil produced by the septum decreases as a function of caudal trim of the sepal cartilage, as would be expected clinically. Lastly, the inferior central portion of the septum near the nasal spine performs a moderate load-bearing role, and these stress values remain consistent in all 3 models.

Displacement of Nasal Cartilage Tissue

All three models demonstrated similar patterns of displacement in response to 5mm nasal tip depression. A surface plot highlighting the movement of the cartilages is illustrated in Figure 6. The intermediate crura were the structures with the greatest displacement (dark red). Interestingly, these structures are slightly anterior to the main load-bearing region, which is located at the medial crural angle bilaterally. It is also important to note the asymmetric displacement of the caudal septum and the major alar cartilages, likely due to the rightward deviation of this subject's caudal septum. As expected, the septal cartilage experienced the greatest displacement principally in the caudal septum (Figure 7).

Recoil Force

The recoil force decreased as more caudal septum was resected from the model, albeit the changes were marginal. In the normal computer model, without any septal resection, the recoil force was −11.66 N. By comparison, the recoil force of a 3mm and 5mm resection decreased to −11.65 N and −11.61 N, respectively.

DISCUSSION

The cost of computation has dropped exponentially over the last decade, and with this trend, finite element modeling has transitioned from supercomputers to the laptop. FEM software is now inexpensive, as are animation and graphics software packages (relatively speaking), providing unprecedented access for biomedical engineers to simulate the behavior of many organs and tissues in the body. This FEM is a first attempt to perform mechanical analysis of the nasal tip, a heterogeneous composite structure, that heretofore has only been described using phenomenological terminology and descriptive analysis[8,15]. While a comprehensive model of nasal behavior is our ultimate goal, we believe that the key first steps have been described with respect to developing such a model with anatomically correct structure, and have provided a starting point to perform parametric analysis. This study demonstrated how a FEM can enhance our understanding of nasal tip support, and in particular identified the caudal septum as an important contributor.

This study focused on examining the role of the caudal septum with respect to how stress is distributed in the nose following simple depression of the tip. Resecting the caudal septum digitally in an FEM is a relatively straightforward task. Classically, moderate resection of the caudal septum is used to both shorten the nose and increase tip rotation in endonasal rhinoplasty maneuvers. It is well known that over-resection leads to a dramatic reduction in tip support as well as the creation of unattractive tip deformities. Hence, nasal tip depression

—an important component of the physical exam—was simulated to assess tip support and to provide insight on the structural consequences of over-resection.

The septum and major alar cartilages were identified as the most important contributors of structural support of the nasal tip. The von Mises stresses were distributed primarily to these two structures and were observed to decrease in response to resection of the caudal septum. As a result of this decrease, external forces due to tip depression dispersed to the surrounding soft tissue envelope and bone. For this simulation, the “dead space” from resected cartilage was filled with soft tissue, which was the primary reason for this redistribution of forces. Within the septum and alar cartilages, von Mises stresses were concentrated to the caudal septum and the junction of the medial and intermediate crura (the medial crural angle), respectively. This distribution is intuitive given that the medial crural angle and the caudal septum are anatomically adjacent to one another other. Thus, based upon this simulation, preserving these two regions in surgery is important to maintain structural support of the nasal tip. Of note, the cartilage structures in all simulations were shown to transmit force to bone with the maximum stresses distributed to nasal bones and nasal spine. Resection of the caudal septum resulted in decreased von Mises stress distribution to bone indicating that the septal cartilage is important for transmitting these forces. These findings are congruent with the principles of contemporary rhinoplasty practice.

Consistent with well-known clinical observations following surgery, we have shown in our models that shortening the caudal septum reduces the total recoil force opposing tip depression. This agreement between our simulations and clinical observation was what we used as a simple validation measure for our FEM. There certainly are limitations to the approach, and at this point, experimental validation is limited due to several factors including the lack of: 1) a mechanical phantom; 2) accurate in vivo mechanical properties nasal soft tissues and cartilage, and; 3) accurate geometry of cartilage shape and orientation information that cannot be extracted from CT scans. Continued refinement of this FEM is our objective; however, this as a multi-year, if not decade-long, endeavor. Near term, we hope to evaluate the performance of the FEM by using a mechanical phantom that mimics the mechanical behavior of the nose under both static and dynamic loading conditions.

In this first application of the finite element method to examine an anatomically detailed nasal model, we used one subject and made broad assumption with respect to material properties to simplify our analysis. The mechanical properties for skin obtained from the literature[14] were used for all soft tissue structures, rather than specifying discrete values for skin, connective tissue, muscle, and fibro-areolar layers of the tip, midvault, and dorsum. All components of the model were assigned linearly elastic mechanical properties and were considered isotropic; in reality, virtually all tissues are viscoelastic and anistropic. Incorporating viscoelastic material properties in the FEM will enhance future versions of this model.

This computational model required creation of the upper lateral, major alar, and septal cartilage geometry using computer-aided design software, since the density of cartilage is indistinguishable from that of soft tissue in CT. This labor-intensive endeavor introduces

subjectivity, as one must infer structure from the shape of the nose and detailed analysis of shape and surface geometry. Additionally, although ligamentous/fascial, musculoaponeurotic, or muscular attachments between cartilaginous substructures are key contributors to nasal tip support, they have not been implemented in the present simulations. Little is known about the material properties and geometry of these structures in vivo, and in the future, creating models that integrate these structures may facilitate a deeper understanding of their potential contributions. Ongoing active research by our laboratory will focus on examining contributions of the major and minor tip support mechanisms as suggested by Tardy et al[8]. This analysis will include the addition of ligamentous attachments and how variations in the shape or form factor of major alar cartilages (i.e., size, shape, thickness, orientation) affect nasal tip stability. We expect that inclusion of ligamentous attachments at the scroll region, for example, would result in a redistribution of stress into the upper lateral cartilage.

There is a broad trend toward individualized medicine embodied most prominently by patient-specific molecular therapies. Patient-specific therapies can apply to surgery as well, and simulation and modeling are key elements. For rhinoplasty, there already exists software that provides surgeons with a means to preoperatively simulate results. Coupling finite element modeling to this process may provide insight into achieving more predictable long-term results. A rhinoplasty surgeon will have the ability to accurately predict the structural and aesthetic consequences of different surgical maneuvers, and to analyze the effects of added synthetic materials (e.g. PDS™ Flexible Plate) or future tissue-engineered constructs. What we attempted here is to develop and demonstrate the first steps in this process and define the pathway needed to achieve this long-term objective.

CONCLUSION

Based on our simulations, resection of the caudal septum resulted in decreased total recoil force opposing tip depression. Additionally, resection reduced the maximum value of von Mises stresses in the septum and alar cartilage resulting in the redistribution of these forces to the soft tissue envelope and bone. Future examinations will include model renderings of different patients, the addition of ligamentous support structures, and exploring the form factor contribution of the major alar cartilages to overall tip support. Lastly, verifying our numerical model with a physical model is also warranted in future investigations.

Acknowledgments

This work was supported by the Department of Defense Deployment Related Medical Research Program (W81XWH-09-1-0602), the National Institutes of Health (DE019026, HL103764, HL105215, EB015890), National Center for Research Resources, and the National Center for Advancing Translational Sciences (UL1 TR000153).

References

1. Westreich RW, Lawson W. The tripod theory of nasal tip support revisited: the cantilevered spring model. Archives of facial plastic surgery. 2008; 10:170–179. [PubMed: 18490543]
2. Han SK, Lee DG, Kim JB, et al. An anatomic study of nasal tip supporting structures. Ann Plast Surg. 2004; 52:134–139. [PubMed: 14745261]

3. Koike T, Wada H, Kobayashi T. Modeling of the human middle ear using the finite-element method. J Acoust Soc Am. 2002; 111:1306–1317. [PubMed: 11931308]
4. Vampola T, Laukkanen AM, Horacek J, et al. Vocal tract changes caused by phonation into a tube: A case study using computer tomography and finite-element modeling. Journal of the Acoustical Society of America. 2011; 129:310–315. [PubMed: 21303012]
5. Gan RZ, Feng B, Sun Q. Three-dimensional finite element modeling of human ear for sound transmission. Ann Biomed Eng. 2004; 32:847–859. [PubMed: 15255215]
6. Lee SJ, Liong K, Lee HP. Deformation of nasal septum during nasal trauma. Laryngoscope. 2010; 120:1931–1939. [PubMed: 20824645]
7. Lee SJ, Liong K, Tse KM, et al. Biomechanics of the deformity of septal L-Struts. Laryngoscope. 2010; 120:1508–1515. [PubMed: 20564665]
8. Tardy, ME.; Brown, RJ. Raven Press. Surgical Anatomy of the Nose.
9. van Essen NL, Anderson IA, Hunter PJ, et al. Anatomically based modelling of the human skull and jaw. Cells Tissues Organs. 2005; 180:44–53. [PubMed: 16088133]
10. Horgan TJ, Gilchrist MD. The creation of three-dimensional finite element models for simulating head impact biomechanics. IJCrash. 2003; 8:353–366.
11. Agache PG, Monneur C, Leveque JL, et al. Mechanical properties and Young's modulus of human skin in vivo. Arch Dermatol Res. 1980; 269:221–232. [PubMed: 7235730]
12. Shapiro EM, Borthakur A, Kaufman JH, et al. Water distribution patterns inside bovine articular cartilage as visualized by 1H magnetic resonance imaging. Osteoarthritis Cartilage. 2001; 9:533–538. [PubMed: 11520167]
13. Jurvelin JS, Buschmann MD, Hunziker EB. Mechanical anisotropy of the human knee articular cartilage in compression. Proc Inst Mech Eng H. 2003; 217:215–219. [PubMed: 12807162]
14. Jia W, Aguilar G, Verkruysse W, et al. Improvement of port wine stain laser therapy by skin preheating prior to cryogen spray cooling: a numerical simulation. Lasers Surg Med. 2006; 38:155–162. [PubMed: 16493663]
15. Anderson JR. A reasoned approach to nasal base surgery. Arch Otolaryngol. 1984; 110:349–358. [PubMed: 6721774]

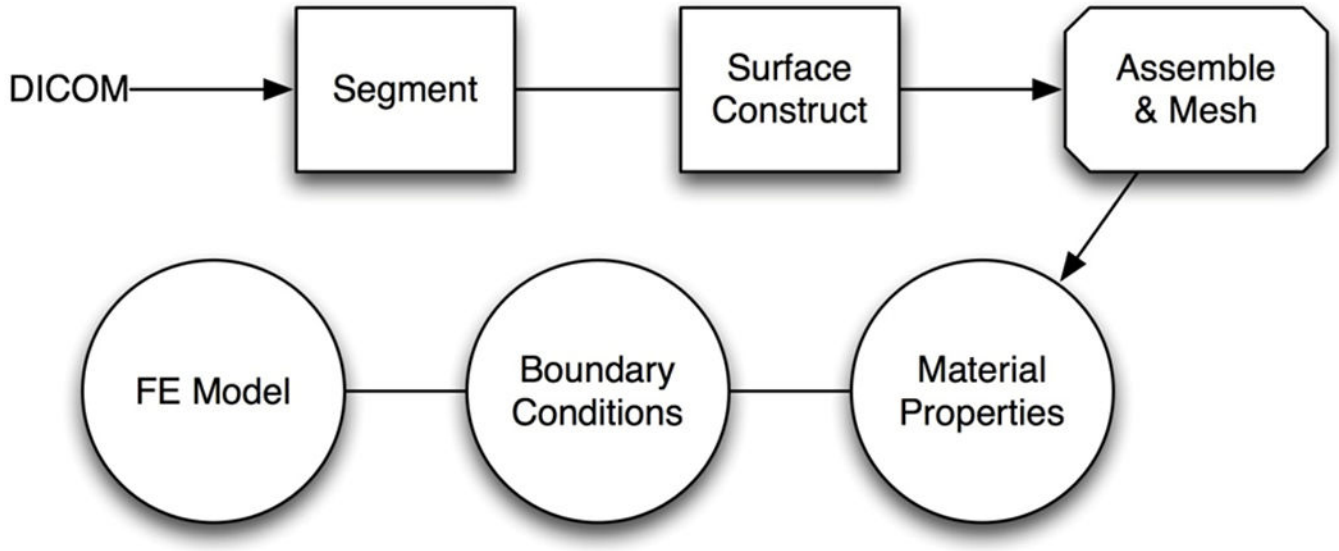

Figure 1.
Overall work flow of the creating the finite element model

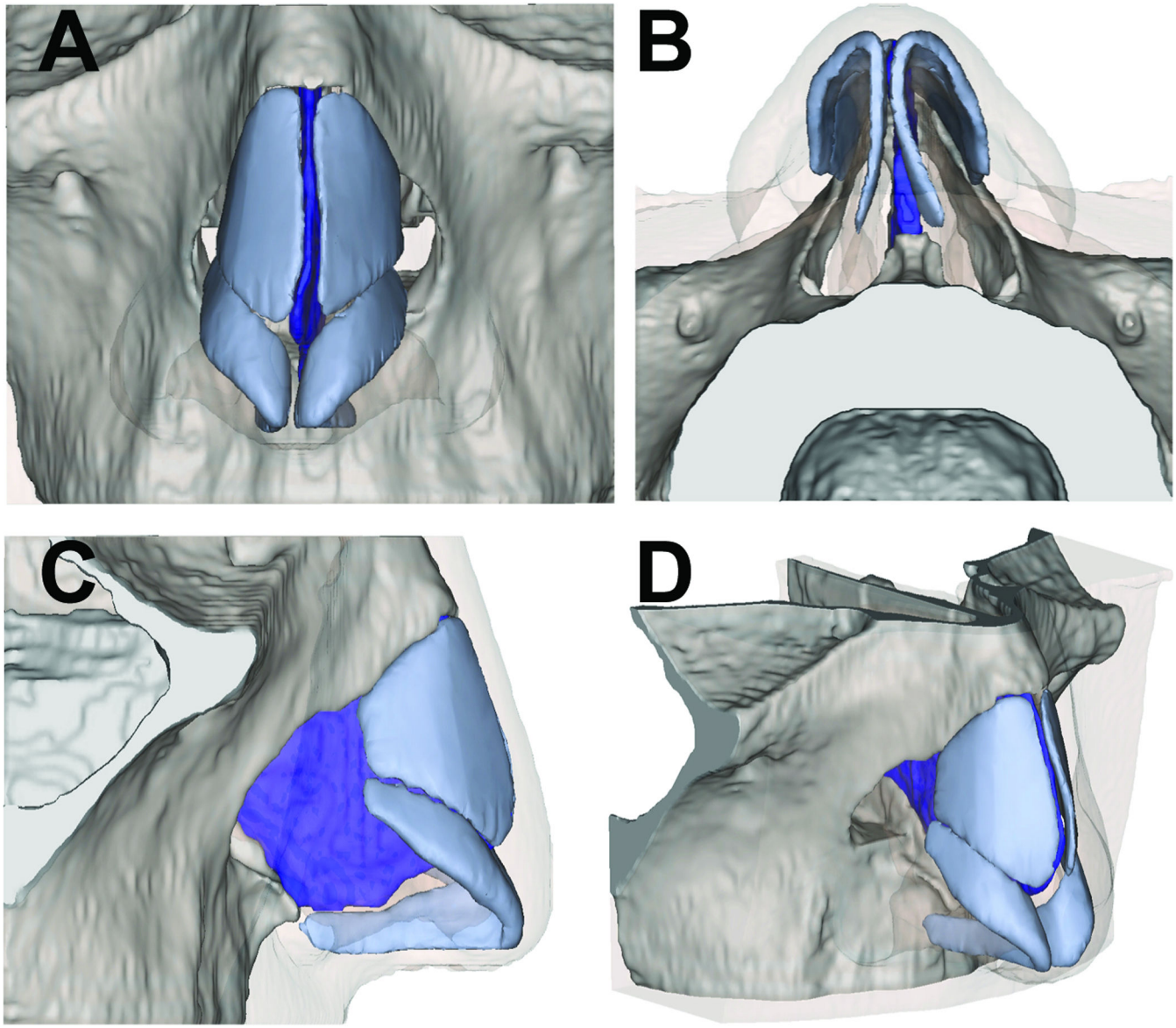

Figure 2.
Rendering of Nasal Model in Mimics
(A) Frontal view (B) Base view (C) Profile view (D) Oblique view

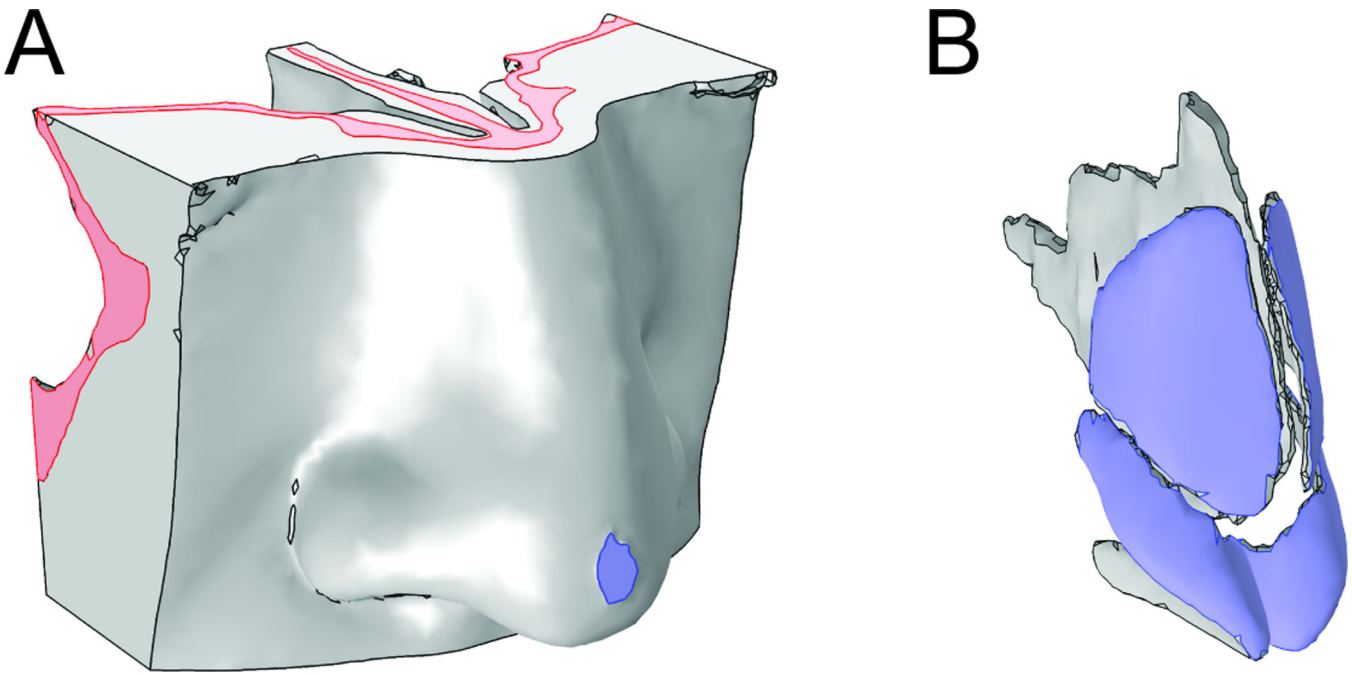

Figure 3.

Boundary conditions in COMSOL

The skull component (pink) is fixed. The 10mm^2 area on the nasal tip (lavender) is subjected to 5mm displacement.

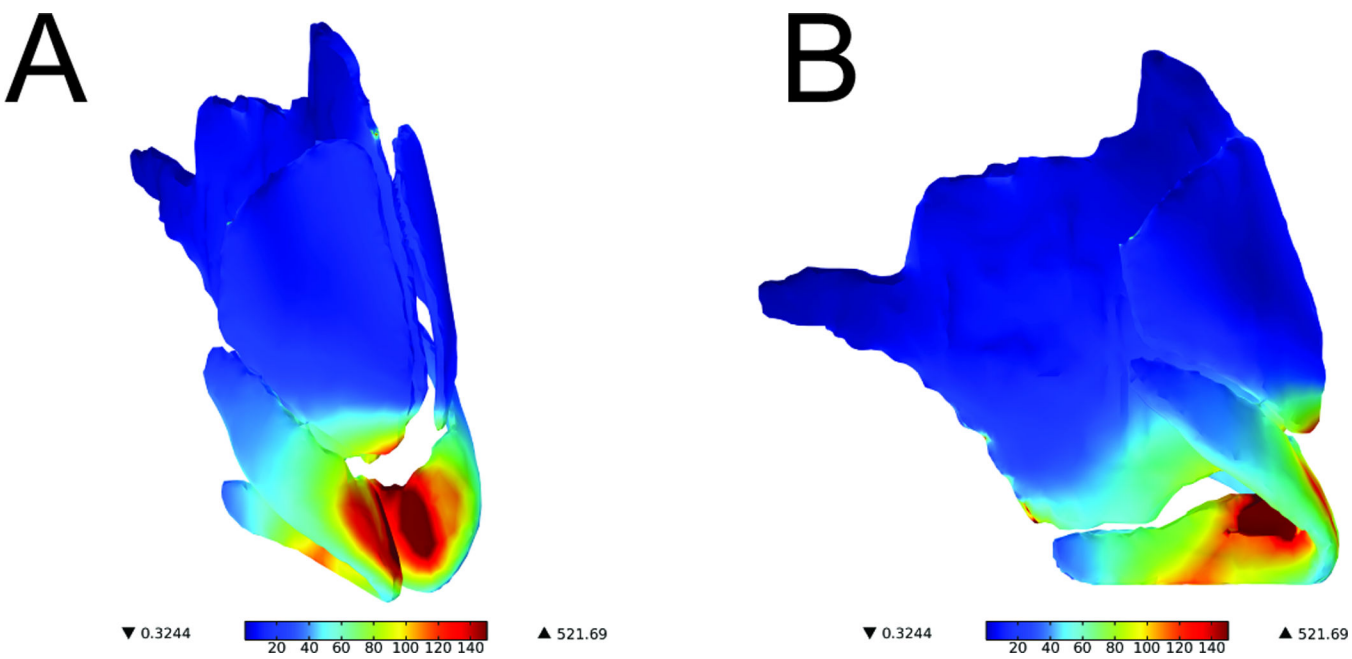

Figure 4.

Surface plot of von Mises stress in cartilage (Normal Model)

Values are represented in kPa. (A) Oblique view (B) Profile view

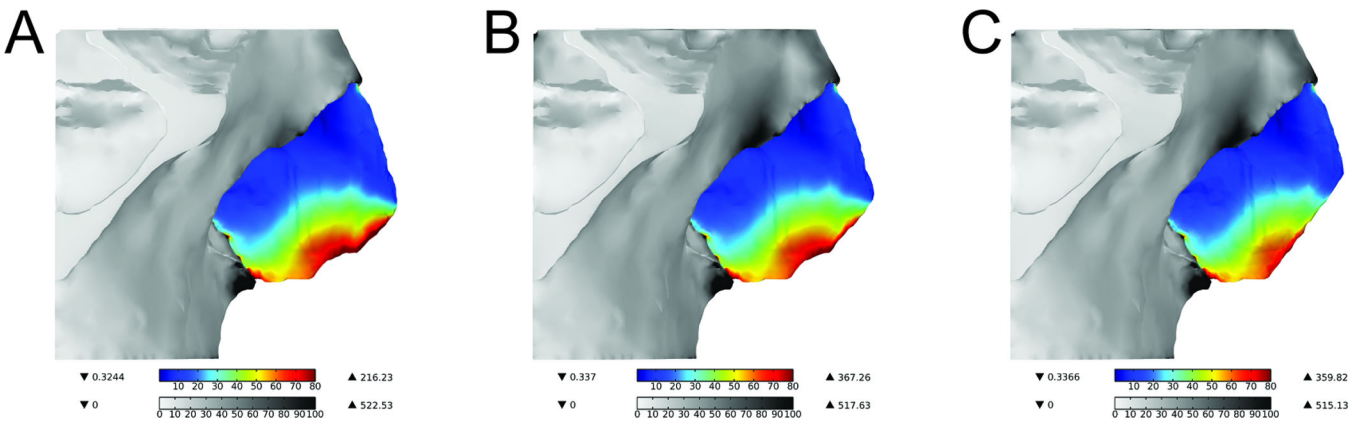

Figure 5.

Surface plot of von Mises stress in bone and septum of all three models

Values are represented in kPa. (A) Normal (B) 3mm caudal septum resection (C) 5mm caudal septum resection

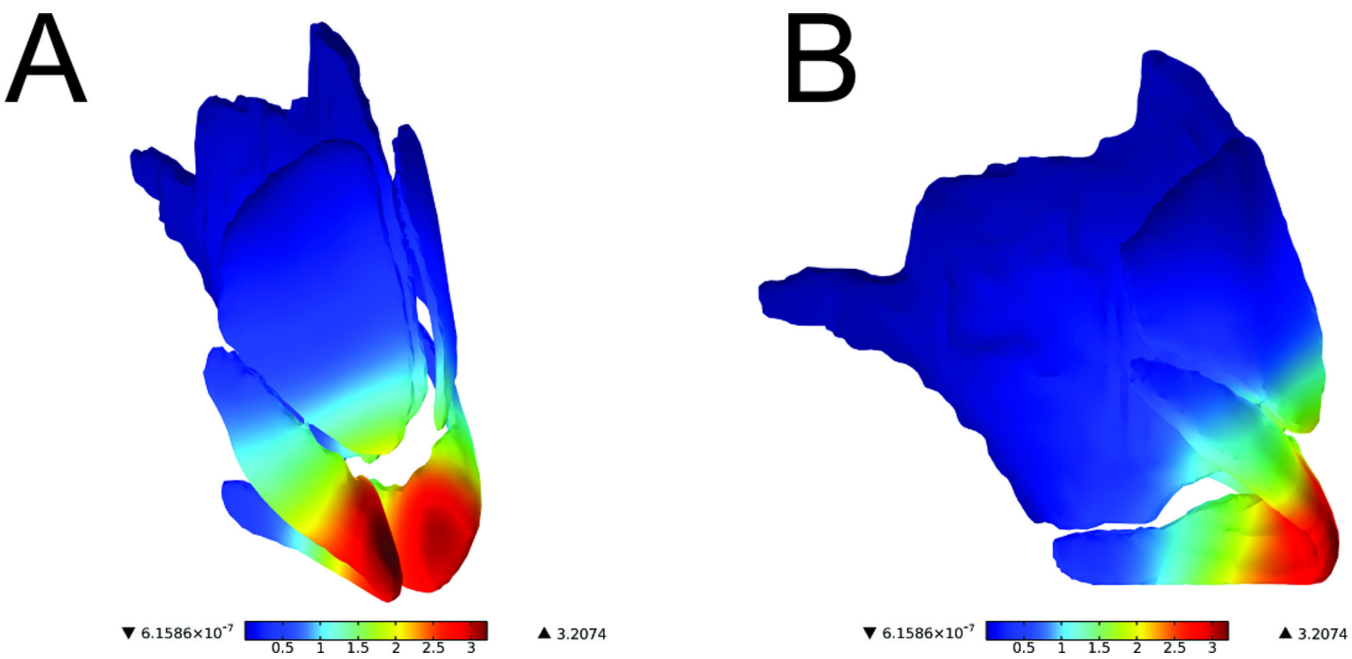

Figure 6.

Surface displacement plot of septum, upper lateral cartilage, and alar cartilage (Normal Model)

Values are represented in mm. (A) Oblique view (B) Profile view

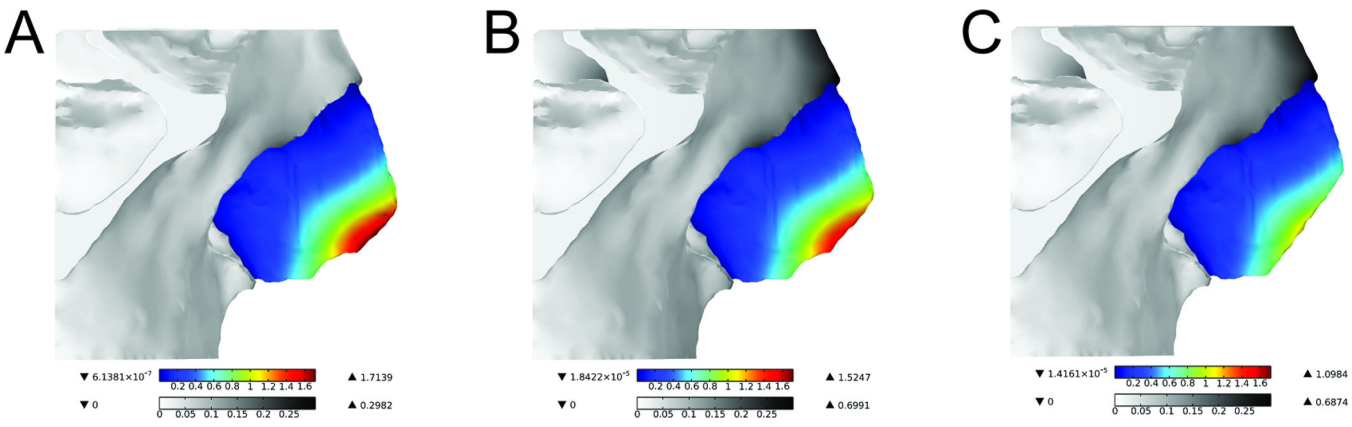

Figure 7.

Surface displacement plot of the bone and septum of all three models

Values are represented in mm. (A) Normal (B) 3mm caudal septum resection (C) 5mm caudal septum resection

Table 1

Material Properties Assignment

Mechanical Property	Skin	Cortical Bone	Cartilage
Density (kg/m^3)	980	1900	1080
Young's Modulus (MPa)	0.5	15000	0.8
Poisson's Ratio (MPa)	0.33	0.22	0.15